NONLINEAR PID CONTROL OF LINEAR PLANTS FOR IMPROVED DISTURBANCE REJECTION

Jinchuan Zheng [*,**] **Guoxiao Guo** [*] **Youyi Wang** [**]

[*] *Data Storage Institute, Singapore 117608, e-mail: Zheng_Jinchuan@dsi.a-star.edu.sg Guo_Guoxiao@dsi.a-star.edu.sg*
[**] *School of EEE, Nanyang Technological University, Singapore 639798, e-mail: EYYWang@ntu.edu.sg*

Abstract: A nonlinear PID (NPID) controller for a class of linear plants with output feedback is studied. The controller gains are modulated by the control error and error rate to yield a closed-loop system for improved disturbance rejection. An optimization problem involving constraints written as linear matrix inequalities (LMIs) is solved to compute the controller parameters. A hard disk drive (HDD) control application shows that the NPID outperforms the conventional PID by 9% in disturbance rejection along with a consequent reduction by 20% in settling time while the stability robustness is maintained.

Keywords: Disturbance rejection, hard disk drive, Lyapunov stability, nonlinear PID control, tracking servo.

1. INTRODUCTION

The proportional-integral-derivative (PID) feedback control is to date the most common structure to deal with the servo problems due to its simplicity. A general linear PID (LPID) control structure is of the form

$$u(t) = k_p e(t) + k_d \frac{de(t)}{dt} + k_i \int_0^t e(\eta) d\eta \qquad (1)$$

where k_p, k_d and k_i are real constant parameters, and $e(t)$ is the control error with $e(t) = r(t) - y(t)$, $r(t)$ and $y(t)$ represents the reference input and the system output, respectively. However, LPID controllers are inherently linear systems and thus are inevitably limited by linear system constraints (Goodwin and Seron, 1997). Therefore, nonlinear PID (NPID) control has received a great deal of attention and it is expected to achieve performance not obtainable by LPID control. Previous studies and applications have attempted to use the NPID control on linear plants to improve tracking accuracy (Xu, *et al.*, 1995), reduce overshoot (Wu, *et al.*, 2004), decrease rise time (Chen, *et al.*, 2003) and compensate for friction (Armstrong, *et al.*, 2001). From the perspective of control laws, NPID control can be categorized into two broad classes (Armstrong, *et al.*, 2001): magnitude-based, those with the controller gains modulated by the control error; and phase-based, those with the controller gains modulated by the control error and error rate explicitly.

The tracking servo in a hard disk drive (HDD) system is referred to as track-following servo, whose objective is to maintain the read/write head as close as possible to the destination track center when the information is being read from or written to the disk. The HDD industry continues to strive for larger capacities on a smaller

form factor. This requires the track width be narrower, which implies a lower error tolerance on the tracking accuracy. Therefore, the track-following servo system is required to efficiently compensate for the disturbances caused by disk vibration, spindle run-out, windage and external vibrations. The task is conventionally fulfilled by a LPID-like compensator (Kobayashi, *et al.*, 1998). Such linear controllers generally have to compromise performance among good disturbance rejection, insensitive to noise, robustness, and so on.

This paper studies the phase-based NPID control of linear plants with output feedback. The selection of the controller parameters is addressed as a linear matrix inequality (LMI) problem, which can be solved efficiently in practice. The HDD system is presented as an example to illustrate the application of the NPID control. The experimental results show that NPID control outperforms LPID control by 9% in disturbance rejection along with a consequent reduction of 20% in settling time while the stability robustness is maintained.

2. NPID CONTROL DESIGN

2.1 System Model in State Space

Consider a linear time-invariant (LTI) and strict proper plant with its state space representation as follows:

$$\begin{cases} \dot{\boldsymbol{x}}(t) = \boldsymbol{A}\boldsymbol{x}(t) + \boldsymbol{B}u(t) + \boldsymbol{G}\boldsymbol{w}(t) \\ y(t) = \boldsymbol{C}_1\boldsymbol{x}(t) + \boldsymbol{D}_1\boldsymbol{w}(t) \\ z(t) = \boldsymbol{C}_2\boldsymbol{x}(t) + \boldsymbol{D}_2\boldsymbol{w}(t) \end{cases} \tag{2}$$

where $\boldsymbol{x}(t) \in \mathbb{R}^n$ is the state vector, $u(t) \in \mathbb{R}$ is the control input, $\boldsymbol{w}(t) \in \mathbb{R}^m$ is the disturbance vector, $y(t) \in \mathbb{R}$ is the measurement output, and $z(t) \in \mathbb{R}$ is the system output, respectively. $\boldsymbol{A}$, $\boldsymbol{B}$, $\boldsymbol{G}$, $\boldsymbol{C}_1$, $\boldsymbol{D}_1$, $\boldsymbol{C}_2$ and $\boldsymbol{D}_2$ are known real constant matrices of appropriate dimensions. The following assumptions on the plant (2) are made.

Assumptions:

(1) The plant is stabilizable with a LPID controller of the form in (1);
(2) Output feedback is used, hence, only $y(t)$ is measurable;
(3) Regulation problem is considered here, that is, $r(t) \equiv 0$.

The LPID controller can be designed using linear control approaches. However, it is well known that the pure differentiator in (1) is not physically implementable because differentiation of the control error containing high frequency noise components will generate large control signal. The problem can be improved by implementing the differentiator as $\frac{s}{\tau_d s+1}$, where τ_d is the time constant with $\tau_d = \frac{0.2}{\omega_0}$, and ω_0 is the desired closed-loop bandwidth (Franklin, *et al.*, 2002). The modified PID controller is then represented in state space as follows:

$$\begin{cases} \dot{\boldsymbol{x}}_c(t) = \boldsymbol{A}_c\boldsymbol{x}_c(t) + \boldsymbol{B}_c e(t) \\ \boldsymbol{y}_c(t) = \boldsymbol{C}_c\boldsymbol{x}_c(t) + \boldsymbol{D}_c e(t) \\ u(t) = \boldsymbol{K}\boldsymbol{y}_c(t) \end{cases} \tag{3}$$

where $\boldsymbol{x}_c = [\tau_d\hat{\dot{e}}(t) - e(t), \int_0^t e(\eta)d\eta]^T \in \mathbb{R}^2$ is the controller state vector, and $\boldsymbol{y}_c(t) = [e(t),\ \hat{\dot{e}}(t),\ \int_0^t e(\eta)d\eta]^T \in \mathbb{R}^3$ is the measurable controller output, and

$$\boldsymbol{A}_c = \begin{bmatrix} -\frac{1}{\tau_d} & 0 \\ 0 & 0 \end{bmatrix}, \boldsymbol{B}_c = \begin{bmatrix} -\frac{1}{\tau_d} \\ 1 \end{bmatrix}, \boldsymbol{C}_c = \begin{bmatrix} 0 & 0 \\ \frac{1}{\tau_d} & 0 \\ 0 & 1 \end{bmatrix},$$
$$\boldsymbol{D}_c = \begin{bmatrix} 1 & \frac{1}{\tau_d} & 0 \end{bmatrix}^T, \boldsymbol{K} = \begin{bmatrix} k_p & k_d & k_i \end{bmatrix}. \tag{4}$$

Folding the controller (3) into the plant (2), then the closed-loop system is given by

$$\begin{cases} \dot{\boldsymbol{x}}_a(t) = \boldsymbol{A}_a\boldsymbol{x}_a(t) + \boldsymbol{G}_a\boldsymbol{w}(t) \\ z(t) = \boldsymbol{C}_{2a}\boldsymbol{x}_a(t) + \boldsymbol{D}_2\boldsymbol{w}(t) \end{cases} \tag{5}$$

where $\boldsymbol{x}_a(t) = [\boldsymbol{x}_c^T, \boldsymbol{x}^T]^T \in \mathbb{R}^{n+2}$ is the augmented state vector; and

$$\boldsymbol{A}_a = \left[\begin{array}{c|c} \boldsymbol{A}_c & -\boldsymbol{B}_c\boldsymbol{C}_1 \\ \hline \boldsymbol{B}\boldsymbol{K}\boldsymbol{C}_c & \boldsymbol{A} - \boldsymbol{B}\boldsymbol{K}\boldsymbol{D}_c\boldsymbol{C}_1 \end{array}\right] \tag{6}$$

is the augmented closed-loop system matrix;

$$\boldsymbol{G}_a = \left[\begin{array}{c} -\boldsymbol{B}_c\boldsymbol{D}_1 \\ \hline \boldsymbol{G} - \boldsymbol{B}\boldsymbol{K}\boldsymbol{D}_c\boldsymbol{D}_1 \end{array}\right] \tag{7}$$

is the augmented disturbance input vector; and

$$\boldsymbol{C}_{2a} = [\boldsymbol{\phi}, \boldsymbol{C}_2] \tag{8}$$

is the augmented system output vector, $\boldsymbol{\phi} \in \mathbb{R}^2$ is the zero vector.

Here, the closed-loop system matrix $\boldsymbol{A}_a$ is a function of the controller gain vector $\boldsymbol{K}$; it is however fixed once $\boldsymbol{K}$ is determined. Hence, the system performance is unchangeable online. In the next section, a NPID controller with a time-varying $\boldsymbol{K}(\cdot)$ is presented to yield a closed-loop system for improved disturbance rejection.

2.2 NPID Control Law

Our objective is to design a NPID control law that will maintain the system output closer to zero under the influence of disturbances. This can be accomplished by shifting the constant controller

gain vector $\boldsymbol{K}$ in (4) into a time-varying controller gain vector

$$\boldsymbol{K}(\cdot) = \left[\, k_p(\cdot)\ k_d(\cdot)\ k_i \,\right] \tag{9}$$

such that the closed-loop system dynamics is instantly changed for favorable disturbance rejection. The NPID control law studied here is motivated by that in Xu, *et al.* (1995). More specifically, $\boldsymbol{K}(\cdot)$ is modulated according to whether the system output is moving away from or toward the desired target:

(1) Movement away from the target: $k_d(\cdot)$ decreases while $k_p(\cdot)$ increases to provide high stiffness;
(2) Movement towards the target: $k_p(\cdot)$ decreases while $k_d(\cdot)$ increases to provide high damping.

The NPID control law is illustrated in Fig. 1. The improvement of the NPID control on disturbance rejection can be qualitatively explained as: at the shaded areas the higher control gain acts as a stiff spring to constrain the system output moving away from the target; while at the non-shaded areas the lower gain and higher damping act as an energy absorber to remove the energy from the overall system. Thus, the NPID control benefits from the nonlinear controller gains and achieves higher disturbance rejection than that under LPID control.

A nonlinear gain vector function $\boldsymbol{K}(\cdot)$ satisfying the NPID control law above can be constructed as follows:

$$k_p(\cdot) = k_p[1 + \nu\alpha\rho(e, \hat{e})] \tag{10}$$

$$k_d(\cdot) = k_d[1 - (1-\nu)\alpha\rho(e, \hat{e})] \tag{11}$$

$$\rho(e, \hat{e}) = \begin{cases} 1 & \text{if } e(t)\hat{e}(t) > 0 \\ 0 & \text{if } e(t)\hat{e}(t) = 0 \\ -1 & \text{if } e(t)\hat{e}(t) < 0 \end{cases} \tag{12}$$

where $\nu \in [0, 1]$ is the weighting factor indicating the extent to which the nonlinear gain affects k_p and k_d, respectively; and $\alpha \in [0, \min(\frac{1}{\nu}, \frac{1}{1-\nu})]$ is the tuning parameter which determines the range of the nonlinear gain and assures the gain invariably positive. It is desired that α be maximized for best performance improvement. This will be illustrated later with an example shown in Fig. 2.

Combining (10)–(12) into (5) gives a nonlinear closed-loop system of the form

$$\begin{cases} \dot{\boldsymbol{x}}_a(t) = \boldsymbol{A}_N(\rho)\boldsymbol{x}_a(t) + \boldsymbol{G}_N(\rho)\boldsymbol{w}(t) \\ z(t) \ = \boldsymbol{C}_{2a}\boldsymbol{x}_a(t) + \boldsymbol{D}_2\boldsymbol{w}(t) \end{cases} \tag{13}$$

where

$$\boldsymbol{A}_N(\rho) = \boldsymbol{A}_a + \alpha\boldsymbol{A}_\Delta(\rho) \tag{14}$$

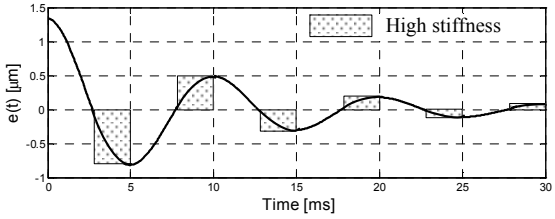

Fig. 1. Illustration of NPID control, adapted from Xu, *et al.* (1995).

$$\boldsymbol{A}_\Delta(\rho) = \left[\begin{array}{c|c} \boldsymbol{\phi} & \boldsymbol{\phi} \\ \hline \boldsymbol{B}\boldsymbol{K}_\Delta(\rho)\boldsymbol{C}_c & -\boldsymbol{B}\boldsymbol{K}_\Delta(\rho)\boldsymbol{D}_c\boldsymbol{C}_1 \end{array}\right] \tag{15}$$

$$\boldsymbol{K}_\Delta(\rho) = \left[\, k_p\nu\rho,\ -k_d(1-\nu)\rho,\ 0 \,\right] \tag{16}$$

2.3 Selection of NPID Controller Parameters Using an LMI Approach

For the derived NPID control system (13), suppose a linear gain vector $\boldsymbol{K}$ has been designed to assure $\boldsymbol{A}_a$ stable and ν is known, then a question naturally arises: how to select the maximum α that assures the nonlinear closed-loop system asymptotically stable. The problem can be solved analytically for a low order system. For example, consider a second-order plant of the form

$$\boldsymbol{A} = \begin{bmatrix} 0 & 1 \\ a_1 & a_2 \end{bmatrix}, \boldsymbol{B} = \begin{bmatrix} 0 \\ 1 \end{bmatrix}, \boldsymbol{C} = \begin{bmatrix} 1\ 0 \end{bmatrix}. \tag{17}$$

Assume both states of the plant are measurable and the NPD control in (10)–(12) is applied. Then the nonlinear closed-loop system is derived by

$$\begin{cases} \dot{x}_1 = x_2 \\ \dot{x}_2 = [a_1 - k_p(\cdot)]x_1 + [a_2 - k_d(\cdot)]x_2. \end{cases} \tag{18}$$

To study the stability condition of the system, a natural Lyapunov function candidate may be taken as the energy-like function

$$V(\boldsymbol{x}) = \int_0^{x_1} [k_p(\cdot) - a_1]y dy + \frac{1}{2}x_2^2. \tag{19}$$

Let $k_p(\cdot) > a_1$, then $V(\boldsymbol{x})$ is positive definite and

$$\begin{aligned} \dot{V}(\boldsymbol{x}) &= [k_p(\cdot) - a_1]x_1x_2 + x_2\dot{x}_2 \\ &= -[k_d(\cdot) - a_2]x_2^2. \end{aligned} \tag{20}$$

Given that $k_d(\cdot) > a_2$, $\dot{V}(\boldsymbol{x})$ is negative definite. Hence, the maximum α satisfying the stability condition is simply derived as

$$\alpha = \min\{\frac{1}{\nu}, \frac{1}{1-\nu}, \frac{k_p - a_1}{\nu k_p}, \frac{k_d - a_2}{k_d - \nu k_d}\}. \tag{21}$$

A numerical simulation of the example was carried out. The parameters are selected as: $a_1 = -10^5$,

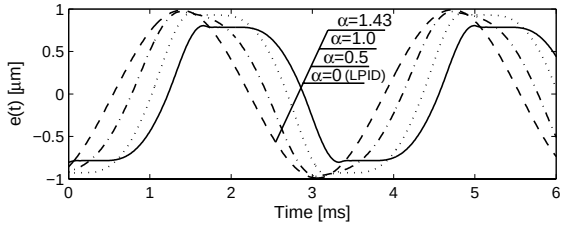

Fig. 2. Simulation result: disturbance rejection improved when α increases.

$a_2 = -180$, $k_p = 10^7$, $k_d = 10^3$, $\nu = 0.7$ and output disturbance source = $2\sin(2\pi 300t)$. Thus, from (21), it follows that

$$\alpha = \min\{1.43, 3.33, 1.44, 3.93\} = 1.43 \qquad (22)$$

The simulation result in Fig. 2 shows that disturbance rejection is gradually improved when α increases within the region that satisfies the stability conditions.

However, for a high order system the stability problem becomes extremely complicated and no systematic methods are available to find appropriate Lyapunov functions that satisfy the stability conditions. But note that the proposed NPID control system (13) is essentially switched among three linear subsystems as follows:

$$\boldsymbol{A}_N(\rho) = \begin{cases} \boldsymbol{A}_a + \alpha\boldsymbol{A}_{\Delta 1} & \text{if } \rho = 1 \\ \boldsymbol{A}_a + \alpha\boldsymbol{A}_{\Delta 2} & \text{if } \rho = 0 \\ \boldsymbol{A}_a + \alpha\boldsymbol{A}_{\Delta 3} & \text{if } \rho = -1 \end{cases} \qquad (23)$$

Therefore, a sufficient stability condition presented by Johansson and Rantzer (1998) can be applied to the system (13) directly and restated as follows:

Proposition 1: The NPID control system (13) is exponentially stable if there exists a common matrix $\boldsymbol{P} = \boldsymbol{P}^T > 0$ for all the subsystems in (23) such that

$$(\boldsymbol{A}_a + \alpha\boldsymbol{A}_{\Delta i})^T\boldsymbol{P} + \boldsymbol{P}(\boldsymbol{A}_a + \alpha\boldsymbol{A}_{\Delta i}) < 0, \quad i = 1, 2, 3. \qquad (24)$$

The above proposition can be proved using a globally quadratic Lyapunov function $V(\boldsymbol{x}) = \boldsymbol{x}^T\boldsymbol{P}\boldsymbol{x} > 0$ and thus $\dot{V}(\boldsymbol{x})$ satisfies (24). Then the system (13) is exponentially stable for every trajectory in the state space.

Consequently, finding the maximum α that assures the stability condition in *Proposition 1* can be formulated as an optimization problem involving constraints written as LMIs (Boyd, *et al.*, 1994). The solution of the LMI problem is then equivalent to solving a convex optimization problem. The remarkable advantage here is that efficient software (Gahinet, *et al.*, 1995) is already available to provide reliable numerical solutions. Therefore, the following LMI problem gives the conditions for the existence of the optimal α.

LMI Problem: Given the known matrices $\boldsymbol{A}_{\Delta i}$ and stable $\boldsymbol{A}_a$, the maximum α that assures the NPID control system (13) exponentially stable is the solution of the following optimization problem in the symmetric matrix $\boldsymbol{P}$ and scalar α:

$$\text{maximize} \quad \alpha \qquad (25)$$

subject to

$$\begin{aligned} &\boldsymbol{P} > 0, \quad 0 \le \alpha \le \min(\frac{1}{\nu}, \frac{1}{1-\nu}), \\ &\boldsymbol{A}_a^T\boldsymbol{P} + \boldsymbol{P}\boldsymbol{A}_a + \alpha(\boldsymbol{A}_{\Delta i}^T\boldsymbol{P} + \boldsymbol{P}\boldsymbol{A}_{\Delta i}) < 0, \\ &i = 1, 2, 3. \end{aligned} \qquad (26)$$

Remark: To speed up the computation, $\alpha = \min(\frac{1}{\nu}, \frac{1}{1-\nu})$ can be set as an initial point. If there exists a $\boldsymbol{P}$ satisfying (26), no more iterations are required. The undesirable case happened when $\alpha = 0$ because the NPID control reduces to LPID control. Thus, there always exists a $\boldsymbol{P}$ satisfying (26) because $\boldsymbol{A}_a$ is stable.

2.4 Design Procedure

From the results obtained, the design procedure for the NPID controller (9) can be summarized as the following steps:

(1) Design a LPID controller (3) for the plant (2) using an appropriate method such that the resulting closed-loop system (5) has necessary stability margin and sensitivity magnitude for disturbance rejection.
(2) Replace the LPID controller gains in (5) with the NPID controller gains (10)–(12) such that (13) is obtained. Rewrite (14) as (23).
(3) Select ν according to the disturbance characteristics, e.g., if the disturbance spectrum is more intensive below the open-loop crossover, then $\nu > 0.5$ is suggested because k_p improves the disturbance rejection within this range more effectively than k_d. Substitute ν into $\boldsymbol{A}_{\Delta i}$ and thus the matrices $\boldsymbol{A}_a$ and $\boldsymbol{A}_{\Delta i}$ are known. Find the maximum α by solving the LMI problem (26). By far, the NPID controller (9) is found with the nonlinear gains given in (10)–(12).

To smooth the transition among the nonlinear controller gains and thus reduce chattering, the switching function (12) can be implemented with an approximating function as follows:

$$\rho(e, \hat{e}) = \frac{\exp[\beta e \text{sgn}(\hat{e})] - 1}{\exp[\beta e \text{sgn}(\hat{e})] + 1} \qquad (27)$$

where the constant β indicates the switching rate, and it is determined by the order of magnitude of

e such that $\rho(\cdot)$ has a fast switch to ensure the improvement of performance.

3. APPLICATIONS TO HDD SERVO SYSTEMS

3.1 Dynamic Model of HDD

The voice coil motor (VCM) actuator in a HDD, that is, the controlled object, consists of the VCM, arm carriage, the suspension, the slider, and the magnetic head. The control input u is a voltage to the VCM driver. The control variable is the position error signal (PES), which is the relative error between the head positioning y and the servo sectors prewritten on the disk surface. The transfer function of the VCM actuator can be represented as follows:

$$G(s) = \frac{Y(s)}{U(s)} = \frac{k}{s^2} \frac{w_n^2}{s^2 + 2\zeta w_n s + w_n^2} \tag{28}$$

where k is the loop gain, w_n is the resonance natural frequency, and ζ is the damping ratio. A state-space model corresponding to the transfer function can be given by

$$\begin{cases} \dot{\boldsymbol{x}} = \begin{bmatrix} 0 & k & 0 & 0 \\ 0 & 0 & 1 & 0 \\ 0 & 0 & 0 & w_n \\ 0 & 0 & -w_n & -2\zeta w_n \end{bmatrix} \boldsymbol{x} + \begin{bmatrix} 0 \\ 0 \\ 0 \\ w_n \end{bmatrix} u \\ y = \begin{bmatrix} 1 & 0 & 0 & 0 \end{bmatrix} \boldsymbol{x} \end{cases} \tag{29}$$

For the HDD studied here, the parameters of the model are $k = 2 \times 10^6$, $\zeta = 0.12$, and $w_n = 2\pi 5800$ rad/sec.

3.2 NPID Control of HDD Track-following System

The NPID control is applied to the HDD track-following servo system to provide precise head positioning. The controller is designed following the procedure presented in Section 2.4.

Firstly, using the loop shaping techniques, the LPID controller (3) for the VCM actuator (29) is obtained with the parameters:

$$k_p = 15, k_d = 0.003, k_i = 1500, \tau_d = 3 \times 10^{-5}.$$

The system specifications are derived as: phase margin 45 deg, gain margin 10 dB, and open-loop bandwidth 1.2 kHz.

Secondly, construct the NPID control system (13) for the HDD system.

Finally, select $\nu = 0.7$ since disturbances with low and midrange frequencies are more concerned in our study. Solving the corresponding LMI problem (26) gives $\alpha = 1.2$ and a positive definite solution $\boldsymbol{P}$ that guarantees the system stability. Hence, the NPID controller is as follows:

$$k_p(\cdot) = 15[1 + 0.84\rho(e, \hat{e})],$$
$$k_d(\cdot) = 0.003[1 - 0.36\rho(e, \hat{e})].$$

Moreover, the switching function $\rho(e, \hat{e})$ is implemented with (27). In the HDD servo, the order of PES magnitude is nanometer, thus, a typical $\beta = 3 \times 10^8$.

3.3 Experimental Results

The NPID controller was implemented on the actual VCM actuator and compared with the LPID controller by setting $\alpha = 0$. Fig. 3 and 4 show the experimental results for repeatable runouts (RROs) compensation. The RROs correspond to the harmonic disturbances generated by a 7200 RPM spindle. The results show that NPID control obtains higher attenuation for midrange frequency RROs but little for high frequency RROs. Fig. 5 shows the result of the compensation for non-repeatable runout (NRRO) dominated by disk flutter modes. The PES spectrum indicates a 9% reduction of PES 3σ under NPID control. Fig. 6 shows the transient response to step output

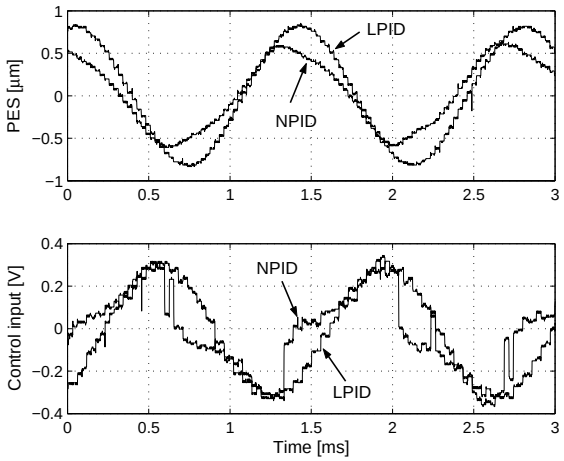

Fig. 3. Compensation for RRO with magnitude = 1 μm and frequency = 720 Hz.

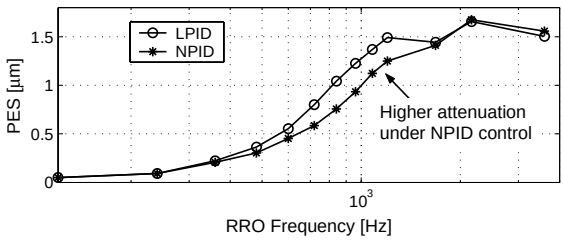

Fig. 4. Summary of RRO compensation tests with RRO magnitude = 1 μm and frequency = 120–3600 Hz.

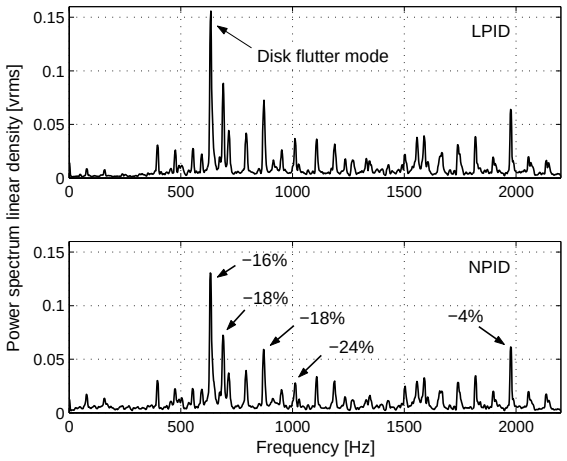

Fig. 5. Compensation for NRRO: 9% reduction of PES 3σ under NPID control compared with LPID control.

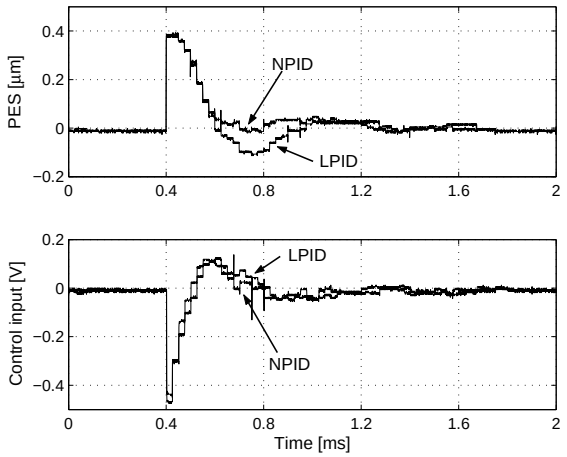

Fig. 6. Step (0.4 μm) output disturbance response: 20% reduction of settling time under NPID control compared with LPID control.

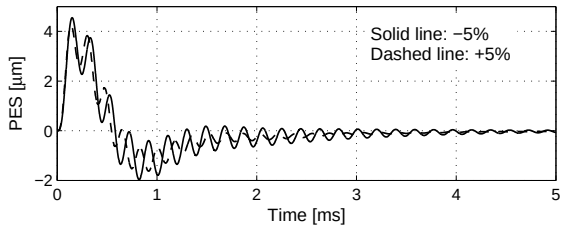

Fig. 7. Simulated impulse input disturbance response with actuator resonance frequency w_n variations ($\pm 5\%$) under NPID control.

disturbance. The result shows that NPID control reduces the overshoot and consequently decreases settling time from 0.5 ms to 0.4 ms, which is a 20% reduction ratio.

Finally, the stability robustness is evaluated under NPID control. Fig. 7 shows that PESs still decay to zero even with actuator resonance frequency variation of $\pm 5\%$.

4. CONCLUSION

A NPID controller has been presented to improve disturbance rejection. The selection of the controller parameter is formulated as an optimization problem with constraints written as LMIs, which can be solved efficiently by the convex programming techniques. The HDD control application shows that NPID control outperforms LPID control by 9% in disturbance rejection along with a consequent reduction by 20% in settling time while maintaining stability robustness. Future research will explore control design methods that ensure the performance goals directly.

REFERENCES

Armstrong, B., D. Neevel and T. Kusik (2001). New results in NPID control: tracking, integral control, friction compensation and experimental results. *IEEE Trans. Contr. Syst. Technol.* **9**(2), 399–406.

Boyd, S., L. Ghaoui, E. Feron and V. Balakrishnan (1994). *Linear Matrix Inequalities in System and Control Theory.* Philadelphia, PA: SIAM.

Chen, B. M., T. H. Lee, K. Peng and V. Venkataramanan (2003). Composite nonlinear feedback control for linear systems with input saturation: theory and an application. *IEEE Trans. Automat. Contr.* **48**(3), 427–439.

Franklin, G. F., J. D. Powell and A. Emami-Naeini (2002). *Feedback Control of Dynamic Systems, Fourth Edition.* Prentice Hall.

Gahinet, P., A. Nemirovski, A. J. Laub and M. Chilali (1995). *LMI Control Toolbox for Use with Matlab:* Mathworks.

Goodwin, G. and M. Seron (1997). Fundamental design trade-offs in filtering, prediction and smoothing. *IEEE Trans. Automat. Contr.* **42**(9), 1240–1251.

Johansson M. and A. Rantzer (1998). Computation of piecewise quadratic Lyapunov functions for hybrid systems. *IEEE Trans. Automat. Contr.* **43**(4), 555–559.

Kobayashi, K., S. Nakagawa, T. Atsumi and T. Yamaguchi (1998). High bandwidth servo control designs for magnetic disk drives. In: *IEEE/ASME Int. Conf. Advanced Intelligent Mechatronics.* pp. 3038–3042.

Wu D., G. Guo and Y. Wang (2004). Reset integral-derivative control for HDD servo systems. submitted to *IEEE Trans. Contr. Syst. Technol.*

Xu, Y., J. Hollerbach and D. Ma (1995). A nonlinear PD controller for force and contact transient control. *IEEE Contr. Syst. Mag.* **15**(1), 15–21.